Measurement of Critical Currents of Superconducting Aluminum Nanowires in External Magnetic Fields: Evidence for a Weber Blockade

Tyler Morgan-Wall, Benjamin Leith, Nikolaus Hartman, Atikur Rahman, and Nina Marković

Phys. Rev. Lett. **114**, 077002 — Published 18 February 2015

DOI: 10.1103/PhysRevLett.114.077002

Weber blockade in superconducting nanowires

Tyler Morgan-Wall, Benjamin Leith, Nikolaus Hartman, Atikur Rahman, and Nina Marković
Department of Physics and Astronomy, Johns Hopkins University, Baltimore, Maryland 21218, USA.

We have studied the critical current as a function of magnetic field in short and narrow superconducting aluminum nanowires. In the range of magnetic fields in which vortices can enter a nanowire in a single row, we find regular oscillations of the critical current as a function of magnetic field, with each oscillation corresponding to adding a single vortex to the nanowire. In this regime, the nanowires behave as quantum dots for vortices. As a function of current and magnetic field, we find diamond-shaped regions in which the resistance is zero and the number of vortices is fixed.

Vortices in superconductors are topological excitations that carry quantized magnetic flux [1]. The shape of the vortices and the configurations in which they can exist in a superconductor are strongly affected by the dimensions and the geometry of the sample [1–11]. In thin films, in which the penetration depth λ is larger than the film thickness d, vortices are of the Pearl type [2], and are shaped like pancakes. As the width of the film is reduced, vortices in narrow strips arrange themselves in rows [6]. Vortices cannot exist in nanowires that are narrower than the coherence length ξ [12], but if the width of a nanowire is on the order of a few ξ, vortices will be able to enter the nanowire in a single row. If the nanowire is also short enough that the energy difference between the states containing different number of vortices is significant, then an entry and an exit of a single vortex might be visible in transport measurements [7, 9–11]. Using charge-vortex duality [13], nanowires may exhibit Weber blockade for vortices [7], analogous to Coulomb blockade for electrons in quantum dots [14]. In this Letter, we report experimental evidence of Weber blockade in short superconducting aluminum nanowires. We find well defined diamond-shaped regions of zero resistance as a function of the current and magnetic field, which repeat with a periodicity that corresponds to adding a single flux quantum to the nanowire.

The nanowires were fabricated using cold-developer electron-beam lithography [15] (see supplementary information for details on fabrication and measurement [16]). A scanning electron microscope image of an aluminum nanowire and the schematic of the measurement are shown in Fig. 1.a. The nanowires are 25nm thick, 50-100nm wide and range from 1.5-4.5μm in length. The low temperature resistivities are on the order of $10^{-7}\Omega m$, and the residual resistance ratios are about 1.5, yielding estimates for the mean free path on the order of 1nm and the penetration depth λ around $700nm$ [1]. ξ=$27nm$ was estimated from measurements of the upper critical field B_{C2} of wider strips (with a range of ξ=$15-30nm$ obtained using the slope of $B_{C2}(T)$ at T_C, shown in Fig. S1 in the supplementary information [16]). As discussed below, superconductivity in our nanowires is not destroyed at B_{C2}, but at a higher field B_{C3}, as the narrow nanowires exhibit surface superconductivity at the edges [1, 17]. The typical resistance as a function of temperature is shown in Fig. 1.b. and the resistance as a function of magnetic field is shown in Fig. 1. c.

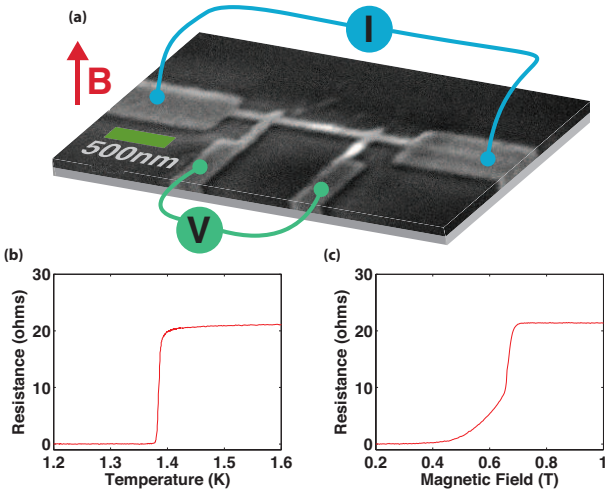

FIG. 1: **(a)** Scanning electron microscope image of an aluminum nanowire. The scale bar is 500nm long. All nanowires are 25nm thick. The nanowire on the image is 70nm wide and 1.5μm long between the current leads (750nm between the voltage leads). The width of other measured nanowires ranges between 50nm and 100nm, and the length ranges between 1.5μm to 4.5μm as measured between the current leads. The resistance measurements are carried out in a four-probe configuration, as shown, and the magnetic field is applied in a direction perpendicular to the plane of the substrate. **(b)** Resistance as a function of temperature for one of the 1.5μm long nanowires (as shown in Fig. 1.a). The normal state resistance R_N is 20Ω and the T_C is 1.38K. **(c)** Resistance as a function of magnetic field for the same nanowire, measured at 250mK.

The current-voltage characteristics as a function of magnetic field for a 1.5μm long nanowire at 250mK are shown in Fig 2.a. At low fields and low currents, the nanowire is in the superconducting state and the measured voltage is zero. When the current reaches the critical value of I_C, a sharp transition to the normal state is observed (I_C signifies the onset of non-zero resistance). The voltage is shown as a function of increasing current (hysteresis due to Joule heating [18] is shown in Fig. S2 in the supplementary information [16]) . As the mag-

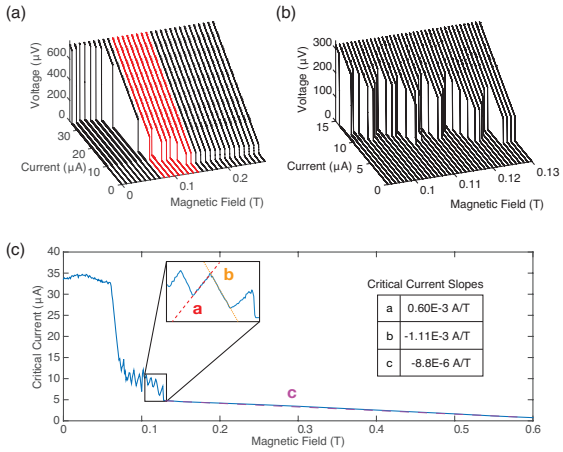

FIG. 2: **(a)** Voltage (vertical axis) as a function of current measured at different discrete values of magnetic field from 0 to 270mT for a 1.5μm long nanowire at 250mK. Each line is a measurement of voltage as a function of applied current at a constant magnetic field. **(b)** Current-voltage characteristics in the range of magnetic fields between 90 and 130mT, where the critical current shows non-monotonic behavior as a function of magnetic field. **(c)** Critical current as a function of magnetic field for a 1.5μm long wire at 250mK. The inset shows an average over seven high-resolution magnetic field and current scans. The average slopes of three linear regions are listed in the inset.

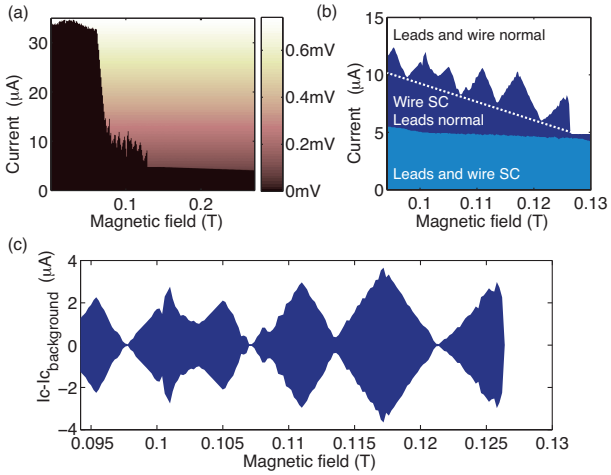

FIG. 3: **(a)** A color plot of the voltage as a function of magnetic field and current at 250mK. The black area is superconducting, and the voltage there is zero. **(b)** A phase diagram as a function of magnetic field and current at 250mK. The boundary between the dark blue and the white region is extracted from seven high-resolution magnetic field sweeps (shown in Fig. S3 in supplementary information [16]). **(c)** The phase diagram as a function of current and magnetic field for a 1.5μm long wire at 250mK in the oscillating regime, with the linear background (shown as a white dashed line in Fig 3. b.) subtracted. The slope of the subtracted portion was chosen to run along the dips of the oscillations and is somewhat arbitrary - it is not meant to be quantitative, but rather intended to highlight the oscillations only. As argued in the main text, this is also an attempt to separate the vortex degrees of freedom (linear increase and decrease of critical current) from the effects of suppressing the superconductivity in the bulk of the wire (approximated as a linear decrease in the range of magnetic fields in which the oscillations are observed). The resistance is zero inside the diamond-shaped regions (blue).

netic field is increased, I_C decreases to a lower value and begins to oscillate, as shown in a close-up in Fig. 2.b.

The critical current as a function of magnetic field for the same nanowire is shown in Fig. 2.c. After the initial drop around 60mT, oscillations in the critical current are clearly visible in the range of magnetic fields between 80-127mT. The inset in Fig. 2.c. shows an average over seven high-resolution magnetic field and current scans (see Fig. S3 in the supplementary information [16]). There is a clear pattern in the critical current as a function of the magnetic field: apart from a few small irregularities, the critical current increases linearly, reaches a peak, and then decreases linearly. This pattern repeats with a periodicity of about 5mT, and it stops abruptly upon reaching a peak at 127mT. Above 127mT, the critical current decreases linearly to zero.

The voltage as a function of magnetic field and the applied current is shown in Fig. 3.a. (data from additional samples are shown in Fig. S4 in the supplementary information [16]). Figure 3.b. shows a phase diagram for the nanowire and the current leads. The resistance of the current leads was measured separately in a four-probe measurement, as shown in Figs. S5 and S6 in the supplementary information [16]. The light blue area represents the values of the currents and magnetic fields at which both the leads and the nanowire are superconducting. As the current is increased, the current leads are driven normal (see Fig S6 in the supplementary information [16]), but the nanowire remains superconducting (dark blue area). We note that the nanowires have a higher T_C and a higher $I_C(0)$ than the leads [19]. The current leads are normal at the current levels at which the critical current oscillations are observed in the nanowire, and the critical current of the leads decreases monotonically with the magnetic field, with no oscillations. We found oscillations in nanowires that were up to 4.5μm long, although they were no longer strictly periodic when the length of the wire exceeded about 2μm. We have not observed any significant asymmetry for the opposite polarity of the magnetic field, nor a hysteresis in I_C with respect to the magnetic field. To highlight the oscillations in I_C, which appear to be superimposed on a background of decreasing critical current as a function of magnetic field, we also show the phase diagram as a function of current and magnetic field in Fig. 3.c. with the background subtracted.

As we argue below, the observed critical current oscil-

lations can be understood in terms of discrete entry and exit of single vortices in the nanowire. The appearance of vortices in thin films of superconductors has been studied extensively, both theoretically [6, 20–29] and experimentally [3, 30–32]. In order to understand the observed oscillations of the critical current in magnetic field, we have to consider the characteristic dimensions of our samples. In thin and narrow strips, where both the thickness and the width are of the order of ξ, the finite size of the vortex core cannot be ignored and one should use the Ginzburg-Landau model [22, 23, 25, 28], rather than the London theory. Within the Ginzburg-Landau model, it has been argued that vortices can enter a thin film strip if its width is at least 1.8ξ [6]. Assuming that the coherence length in our samples is about ξ=27nm, the width of our samples (50-100nm) is just large enough to allow entry of a single row of vortices.

In general terms, the stability of vortices in a superconducting strip is governed by their potential energy, which varies across the width of the strip. The potential energy of a single vortex in the nanowire can be written as follows [7, 20, 22, 23, 33]:

$$E = 2\pi\rho \ln \frac{\sin \pi y/w}{\sin \pi \xi/w} + \frac{4\pi^2 \rho B}{\Phi_0}\left[\left(y - \frac{w}{2}\right)^2 - ... \right. \\ \left. \left(\xi - \frac{w}{2}\right)^2\right] + \frac{\Phi_0 J}{w}\left(y - \frac{w}{2}\right) \quad (1)$$

where y is the coordinate across the width of the wire, w is the width, B is the magnetic field, J is the current density, ρ is the superfluidic stiffness, ξ is the coherence length, and Φ_0 is the flux quantum. The first term is a contribution from the vortex image interaction, where the divergence at the edges is cut off by the finite size of the vortices. The second term arises from the interaction energy between the vortex and the applied magnetic field - this term is responsible for creating a potential well for vortices in the center of the nanowire. The two terms in the square parentheses come from integrating over the distance near the edges in which the current is non-zero [22], which is on the order of $\frac{w}{2} - \xi$, assuming that we only have one vortex in the center of the wire. The third term is the potential from the force that arises from the interaction between the vortex and the applied current - this term tilts the potential towards one edge of the nanowire. The potential energy of a vortex is shown in Fig. 4.a. At low magnetic fields, the potential energy is positive everywhere, and the vortices cannot enter the sample. As the magnetic field is increased to B_0, the potential energy develops a local minimum in the center of the nanowire, but it remains positive everywhere. Upon further increase of the magnetic field to B_S, the potential energy reaches zero in the center of the strip, and becomes negative in higher fields. Above B_S, the vortices can exist in the film in a stable state [20], but potential barriers at the edges [21, 27, 31, 34] will impede the entry

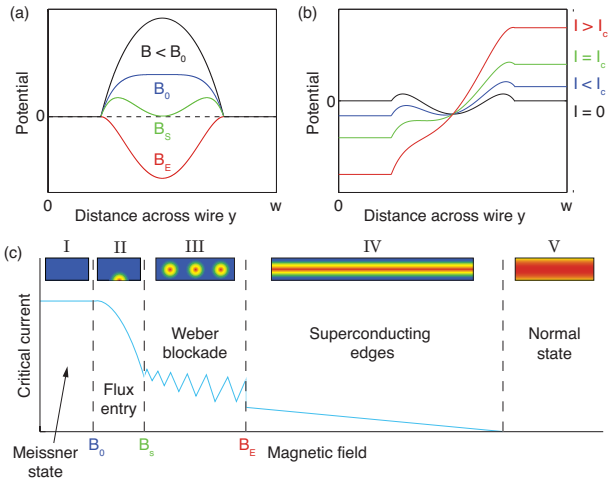

FIG. 4: **(a)** Potential energy of a vortex as a function of its position across the width of the wire for different magnetic fields, with no applied current. At B_0, the potential develops a minimum which reaches zero at B_S. B_E is the field at which the potential barriers at the edges disappear. **(b)** Potential energy of a vortex as a function of its position along the width of the wire for different applied currents in a magnetic field between B_0 and B_S. **(c)** A schematic of different vortex regimes in the nanowire as a function of current and magnetic field. The blue color denotes the superconducting regions and the red color corresponds to the normal regions.

of vortices until a higher magnetic field B_E is reached, at which the potential barriers at the edges disappear. For large enough currents, both barriers disappear, as shown in Fig. 4. b.

Since the vortices need to both enter and exit the nanowire for the resistance to appear, we expect the larger of the two barriers to determine I_C. For a fixed number of vortices in the nanowire, the increasing magnetic field will cause the exit barrier to increase and the entry barrier to decrease, until another vortex can enter the nanowire [6]. If the nanowires are shorter than 100 ξ, this may manifest as oscillations in the critical current [6]. The periodicity observed in shorter nanowires corresponds to $\Phi_0/2\pi$Lw (L is the length and w is the width).

In the regime in which vortices can enter the nanowire, the critical current is determined by the sum of the applied current, vortex current and the screening currents generated in the superconducting regions. After the first vortex enters the nanowire, an increasing magnetic field will generate screening currents in order to expel additional flux. In this regime, the exit barrier is lower than the entry barrier, and the critical current is determined by the entry barrier. The entry barrier decreases with magnetic field [6], causing a decrease in the critical current, $I_C \propto w^2(B_S - B)/4\pi\lambda$ [22]. This continues until the additional flux reaches one half of a flux quantum - the entry barrier now becomes lower than the exit bar-

rier, so the onset of resistance is determined by the exit barrier [6], causing an increase in the critical current, $I_C \propto w^2 B/4\pi\lambda$ [22], in agreement with the observed linear slopes in Fig. 3. c. The cycles repeat until the vortices begin to overlap, and the oscillations stop abruptly at the last local maximum in I_C.

The full phase diagram is shown in Fig. 4. c. Because the width of our nanowires is on the order of ξ (and much smaller than λ), they behave like thin films in a parallel field [1] and I_C is only weakly affected at low fields (region I). At higer fields, I_C starts to decrease (region II). Once the vortices can enter the nanowire, they are arranged in a single row (region III) [6]. As the magnetic field is increased further, the potential barriers at the edges decrease, the vortex row becomes denser, eventually merging into a normal channel in the center of the strip (region IV) [8, 25]. Region IV shows a slow linear decrease in I_C until the magnetic field is large enough to destroy the surface superconductivity at the edges [1, 8, 17] and the sample enters the normal state (region V).

An equivalent description of the Weber blockade regime in Region III can be obtained by considering only the vortex degrees of freedom. Using the vortex-charge duality, our nanowire can be viewed as a vortex analog of a Coulomb-blockaded quantum dot. The magnetic field is the analog of the gate voltage, as it tunes the number of vortices in the nanowire. The applied current is the analog of the bias voltage, as it causes the vortices to cross the nanowire. In the dual picture, zero resistance corresponds to zero conductance for vortices (as illustrated in Fig. 3.c.), in analogy with the Coulomb diamonds in quantum dots, inside which the electron conductance is zero, and the number of electrons is fixed.

We conclude that the number of vortices in narrow and short superconducting nanowires can be precisely tunable by applied magnetic field, which can be used as an advantage in flux-based superconducting devices.

ACKNOWLEDGEMENTS

The authors would like to thank G. Berdiyorov, F. M. Peeters, D. Y. Vodolazov, D. Pekker, and V. Oganesyan for useful comments and suggestions. This work was supported by NSF Grant No. DMR-1106167. N. M. would like to thank the Aspen Center for Physics (through the NSF Grant No. PHYS-1066293) for hospitality.

[1] M. Tinkham, *Introduction to Superconductivity* (McGraw-Hill Inc., 1996).
[2] J. Pearl, Appl.Phys. Lett. **5**, 65 (1964).
[3] V. V. Moshchalkov, L. Gielen, C. Strunk, R. Jonckheere, X. Qiu, C. Van Haesendonck, and Y. Bruynseraede, Nature **373**, 319 (1995).
[4] M. V. Milošević, A. Kanda, S. Hatsumi, F. M. Peeters, and Y. Ootuka, Phys. Rev. Lett. **103**, 217003 (2009).
[5] B. Xu, M. V. Milošević, S.-H. Lin, F. M. Peeters, and B. Jankó, Phys. Rev. Lett. **107**, 057002 (2011).
[6] D. Y. Vodolazov, Phys. Rev. B **88**, 014525 (2013).
[7] D. Pekker, G. Refael, and P. M. Goldbart, Phys. Rev. Lett. **107**, 017002 (2011).
[8] R. Cordoba, T. I. Baturina, J. Sese, A. Yu Mironov, J. M. De Teresa, M. R. Ibarra, D. A. Nasimov, A. K. Gutakovskii, A. V. Latyshev, I. Guillamn, et al., Nat. Comm. **4**, 1437 (2013).
[9] Y. Atzmon and E. Shimshoni, Phys. Rev. B **83**, 220518 (2011).
[10] Y. Atzmon and E. Shimshoni, Phys. Rev. B **85**, 134523 (2012).
[11] A. Johansson, G. Sambandamurthy, D. Shahar, N. Jacobson, and R. Tenne, Phys. Rev. Lett. **95**, 116805 (2005).
[12] N. Markovic, C. N. Lau, and M. Tinkham, Physica C **387**, 44 (2003).
[13] M. P. A. Fisher, Phys. Rev. Lett. **65**, 923 (1990).
[14] C. W. J. Beenakker, Phys. Rev. B **44**, 1646 (1991).
[15] W. W. Hu, K. Sarveswaran, M. Lieberman, and G. H. Bernstein, Journal of Vacuum Science & Technology B **22**, 1711 (2004).
[16] See Supplemental Material at [URL will be inserted by publisher] for additional data.
[17] D. Saint-James and P. G. de Gennes, Phys. Lett. **7**, 306 (1963).
[18] M. Tinkham, J. U. Free, C. N. Lau, and N. Markovic, Phys. Rev. B **68**, 134515 (2003).
[19] J. Romijn, T. M. Klapwijk, M. J. Renne, and J. E. Mooij, Phys. Rev. B **26**, 3648 (1982).
[20] K. K. Likharev, Sov. Radiophys. **14**, 722 (1972).
[21] J. R. Clem, Bull. Am. Phys. Soc. **43**, 411 (1998).
[22] G. Maksimova, Physics of the Solid State **40**, 1607 (1998).
[23] P. Sánchez-Lotero and J. J. Palacios, Phys. Rev. B **75**, 214505 (2007).
[24] E. Bronson, M. P. Gelfand, and S. B. Field, Phys. Rev. B **73**, 144501 (2006).
[25] J. J. Palacios, Phys. Rev. B **57**, 10873 (1998).
[26] G. R. Berdiyorov, X. H. Chao, F. M. Peeters, H. B. Wang, V. V. Moshchalkov, and B. Y. Zhu, Phys. Rev. B **86**, 224504 (2012).
[27] G. M. Maksimova, N. V. Zhelezina, and I. L. Maksimov, Europhys. Lett. **53**, 639 (2001).
[28] I. Aranson, M. Gitterman, and B. Y. Shapiro, Phys. Rev. B **51**, 3092 (1995).
[29] A. V. Kuznetsov, D. V. Eremenko, and V. N. Trofimov, Phys. Rev. B **59**, 1507 (1999).
[30] G. Stan, S. B. Field, and J. M. Martinis, Phys. Rev. Lett. **92**, 097003 (2004).
[31] B. L. T. Plourde, D. J. Van Harlingen, D. Y. Vodolazov, R. Besseling, M. B. S. Hesselberth, and P. H. Kes, Phys. Rev. B **64**, 014503 (2001).
[32] J. Gutierrez, B. Raes, J. Van de Vondel, A. V. Silhanek, R. B. G. Kramer, G. W. Ataklti, and V. V. Moshchalkov, Phys. Rev. B **88**, 184504 (2013).
[33] G. Stejic, A. Gurevich, E. Kadyrov, D. Christen, R. Joynt, and D. C. Larbalestier, Phys. Rev. B **49**, 1274 (1994).
[34] C. P. Bean and J. D. Livingston, Phys. Rev. Lett. **12**, 14 (1964).